

RESEARCH ARTICLE OPEN ACCESS

Thermo-Mechanical Evaluation of Novel Composite Propellant Formulations Based on Styrene-Ethylene/Butylene-Styrene Block Copolymer

Peter J. Wilkinson¹  | Guillaume Kister¹ | Philip P. Gill^{1,2} ¹Cranfield Defence and Security, Cranfield University, Defence Academy of the United Kingdom, Swindon, UK | ²ROXEL (UK Rocket Motors) Ltd., Kidderminster, UKCorrespondence: Peter J. Wilkinson (p.wilkinson@cranfield.ac.uk)

Received: 27 November 2024 | Accepted: 8 October 2025

Keywords: DMA | solid propellant formulations | strain energy density | tensile testing | thermoplastic elastomer

ABSTRACT

Two novel composite propellant formulations have previously been produced from a binder consisting of the thermoplastic elastomer styrene-ethylene/butylene-styrene (SEBS) and a solid filler, either ammonium perchlorate (AP) or 1,3,5-trinitro-1,3,5-triazinane (RDX). The binder, being a commercially available off-the-shelf polymer, has many advantages over a typical bespoke binder, particularly cost and risk of obsolescence. The thermal and hazard properties have shown potential for these formulations. This paper addresses the mechanical properties over a range of service and storage temperatures, which is important in the safety and durability of a propellant. The glass transition temperatures, as determined by dynamic mechanical analysis (DMA), were found to be influenced by the type of filler and the solids loading. The lower glass transition was seen to increase slightly from -41°C for unfilled SEBS to -39°C (AP/SEB 84/16) with AP as a filler; conversely, it decreased to -45°C (RDX/SEBS 80/20) with RDX. The upper glass transition was found to have decreased from 102°C to around 91°C for all formulations tested. Use of DMA—time temperature superpositioning found that the filler influenced the frequency dependency of the mechanical behaviour. Compared to typical AP composite propellants, both the storage modulus (E') from DMA and Young's modulus (E) from tensile testing were substantially greater. Tensile testing also showed that the strain at maximum stress (ϵ_m) was significantly less. However, the maximum stress (σ_{\max}) was similar. SEBS has shown potential as a binder for a stiffer composite propellant (higher modulus).

1 | Introduction

Important factors when developing a new solid propellant formulation include the ballistic performance, safety in storage and operation and the environmental impacts. When producing a propellant on an industrial scale, the cost and long-term security of supply of the raw ingredients become important factors. National and international legislation, such as International Traffic in Arms Regulations (ITAR) [1] and Registration, Evaluation, Authorisation and Restriction of Chemicals (REACH) [2], are limiting factors on the free use of ingredients in solid propellant

formulations. There is evidence of European firms redesigning their munitions to remove ITAR-restricted components [3]. Despite the environmental advantage of using materials from natural sources, such as cotton linters, the inherent variation of naturally sourced materials could adversely affect their use [4]. Small changes in the specification of the materials can result in long and costly requalification processes for the solid propellant manufacturers.

Solid composite propellants in service today commonly use bespoke cured elastomeric binders based on polyurethane

This is an open access article under the terms of the [Creative Commons Attribution](https://creativecommons.org/licenses/by/4.0/) License, which permits use, distribution and reproduction in any medium, provided the original work is properly cited.

© 2025 The Author(s). *Propellants, Explosives, Pyrotechnics* published by Wiley-VCH GmbH.

TABLE 1 | Comparison of mechanical properties of ammonium perchlorate composite and extruded double base propellants (EDB).

Mechanical properties		-40°C	+20°C	+60 ^a /+70°C ^b
EDB ^a	Strain at maximum stress ($\epsilon_{m,\%}$)	2.8	2.5	8
	Modulus (E, MPa)	1835	439	21
Composite ^b	Strain at maximum stress ($\epsilon_{m,\%}$)	50.5	56.5	54.5
	Modulus (E, MPa)	38.9	3.1	2.0

^aEDB data taken from Davenas [8]; ^b Composite average data taken from Sutton [9].

chemistry. Modern polyurethane binders are made with a prepolymer polyol and chemically cured with an isocyanate, forming urethane cross-linkages. The most widely used polyol is hydroxyl-terminated polybutadiene (HTPB). The size of the solid propellant manufacturing industry is tiny compared to the worldwide plastics/polymer industry. Their influence and buying power are limited, and historically, this has meant that they have regularly experienced material obsolescence problems. The use of commercially available off-the-shelf (COTS) polymers as a binder could provide a resilient and cost-effective approach for the development of new solid propellants. The development of a propellant using a thermoplastic elastomer (TPE) as a binder would have the potential to be recyclable, reducing the environmental impact of the disposal of unused munitions [5]. This is possible because the polymer chains within a TPE are held together with ‘fugitive’ cross-links, which become ineffective when they are heated, enabling the polymer to flow (a thermoplastic). On cooling, these ‘fugitive’ cross-links reform and the polymer regains its rubbery properties [6].

Propellants have viscoelastic properties and, as such, exhibit both viscous and elastic characteristics when undergoing deformation. Propellants need to be stiff enough to resist deformation from forces such as gravity or acceleration, and must be elastic enough when thermally strained and return to their original state once the stress is removed. The mechanical properties of viscoelastic materials such as polymers and solid propellants are dependent on temperature and strain rate. Any change in temperature brings a significant change in the tensile strength, elongation, and elastic modulus of the propellant [7]. Shekhar observed that for each class of propellant, as temperature reduces, the elastic modulus and tensile strength of the propellant increase predictably. However, the elongation is very different between propellant types, with case-bonded composite propellants having a much higher percentage elongation (20%–40%) at low temperatures (-55°C) compared to free-standing grains, such as extruded double base propellants (EDB).

From this, we can conclude that at first, there is no one set of target mechanical properties for a new solid propellant formulation. The strain capability (cold) and modulus (hot) are important values historically, but target specification limits are linked to the design of any future grain or motor. Table 1 gives example values for the two most discussed properties: (i) strain capability of the propellant at cold temperatures, important to ensure the propellant can move and deform without damage; (ii) the modulus or strength of the propellant at hot temperatures, important to ensure the propellant does not deform or slump during hot storage or acceleration.

This research follows on from previous work [10], which reported on the formulation and characterisation of two composite propellant formulations made from a COTS polymer as a binder by means of a resonant acoustic mixer (RAM) slurry process. The binder consisted of thermoplastic elastomer styrene-ethylene/butylene-styrene (SEBS) block copolymer and the solid fillers, ammonium perchlorate (AP) or 1,3,5-trinitro-1,3,5-triazinane (RDX). The SEBS-based formulations exhibited similar theoretical ballistic performance, thermal decomposition and small-scale hazard properties to conventional AP-HTPB-based propellants. This paper discusses the important thermo-mechanical properties of these novel AP/SEBS and RDX/SEBS propellant formulations.

2 | Experimental

2.1 | Materials

Polystyrene-block-poly(ethylene-ran-butylene)-block-polystyrene (SEBS) from Sigma-Aldrich, product number: 200565, CAS number: 66070-58-4, >99% w/w purity, styrene 29% w/w, average $M_w \sim 89,000$ Da by Gel Permeation Chromatography. AP of nominal particle size 200 μm (AP200) and 90 μm (AP90) respectively, from The Falcon Project Ltd., RDX, type A, class 5 (97+% pass through a 45 μm sieve) from QinetiQ plc, Fort Halstead, UK. Toluene, isopropanol and DCM from Fisher Scientific as extra pure, with >99% purity.

Five different propellant formulations were made by a novel slurry process utilising a resonant acoustic mixer to create a moulding powder which was then hot pressed into sheets (60 \times 25 \times c.a. 4 mm). Four with AP and one with RDX as the fillers, see compositions in Table 2. AP/SEBS were made with a typically bimodal mixture of coarse AP (AP200) and fine (AP90) in a 4:3 (w/w) ratio. While RDX/SEBS used a mono-modal finer class 5 RDX. Full details of the production method, as well as compatibility and hazard testing, and thermal analysis, can be found in Wilkinson et al. [10].

Cured hydroxyl-terminated polybutadiene (HTPB) polymer sheets were prepared from HTPB R45M (Cray Valley) prepolymer cured with Desmodur N-100 (aliphatic polyisocyanate). The quantity of prepolymer to curing agent was based on the ratio of alcohol to isocyanate groups being 1:1.1. The HTPB prepolymer (86.1% w/w) was first mixed with the AO-2246 antioxidant (2,2'-Methylenebis(4-methyl-6-tert-butylphenol)) (0.9% w/w) in a centrifugal laboratory mixer (Hauschild SpeedMixer) at 3000 rpm for 5 min. This was followed by the addition of the

TABLE 2 | Composition of novel composite styrene-ethylene/butylene-styrene (SEBS) propellant formulations.

Sample	Composition (% w/w)		
	AP ^a	RDX ^b	SEBS
AP/SEBS (60/40)	60		40
AP/SEBS (70/30)	70		30
AP/SEBS (80/20)	80		20
AP/SEBS (84/16)	84		16
RDX/SEBS (80/20)		80	20

^aAP was a typically bimodal mixture [11] of coarse AP (AP200) and fine (AP90) in a 4:3 (w/w) ratio; ^b class 5 RDX.

curing agent (13.0% w/w) and mixing for a further 2 min at 3000 rpm. The sample was then degassed by placing it under vacuum (*ca.* 1 kPa) for 15 min. It was then injected into warmed (70°C) polytetrafluoroethylene moulds and placed vertically in an oven to cure at 70°C for 7 days.

2.2 | Dynamic Mechanical Analysis

A Perkin Elmer DMA 8000 with liquid nitrogen cooling was used for dynamic mechanical analysis (DMA) measurements. The experiments were performed in a single cantilever geometry, under a dry nitrogen atmosphere. Cuboid testing samples were cut (25 × 6 × 4 mm) using a guillotine fitted with a razor blade; the effective length of the samples was *ca.* 10 mm. For temperature scans, the samples were cooled to the starting temperature (−120°C), then heated to +120°C at a rate of 2°C/min. The storage modulus (E'), loss modulus (E'') and $\tan \delta$ were obtained at frequencies of 1 and 10 Hz with a displacement of 0.050 mm (1.25%). Peak analysis on the loss factor ($\tan \delta$) was performed using STARe v. 15.00 software. For frequency scans (time temperature super-positioning [TTS]), the samples were cooled to about −130°C before being heated at 2°C/min to the first isotherm at −120°C. The instrument then ‘soaked’ at this temperature for 3 min before conducting a frequency scan from 0.1 to 100 Hz at six different frequencies per decade (taking three averages) with a displacement of 0.1 mm (2.5%). Then heated to the next isotherm set at 10°C higher, at 2°C/min. This was repeated until the final temperature of +120°C was reached or the response was too small to be accurately measured by the DMA.

2.3 | Tensile Testing

Uniaxial tensile testing was performed on a Universal Testing System (Zwick 1445, Zwick-Roell) fitted with a 10 kN load cell and wedge grips. Measurements were conducted at −40, +20 and +74°C inside a Zwick liquid nitrogen temperature-controlled chamber. Samples were cut from a pressed sheet using a guillotine fitted with a razor blade, making rectangular test samples *ca.* 50 mm long × 10 mm wide × 4 mm thick. These were clamped *ca.* 20 mm apart using wedge grips. The samples were tested at a strain rate of 42.9 s^{−1} (14.3 mm/min), stress and strain were uncorrected. Strain energies to maximum stress were calculated by finding the area under the stress-strain curve up to the point of greatest stress.

2.4 | Differential Scanning Calorimetry

Thermal analysis was conducted on a Mettler Toledo DSC3+ instrument with liquid nitrogen cooling. Samples (~20 mg) were placed in Mettler Toledo 40 μ L aluminium differential scanning calorimetry (DSC) crucibles with a hole pierced in the lid, allowing the sample to be exposed to the nitrogen atmosphere. All samples apart from unfilled cured HTPB were heated from −130 to 120°C, then cooled back to −130°C. This cycle was then repeated before a final heating to 120°C. Unfilled cured HTPB was heated up to a temperature of 200°C each cycle, instead of 120°C. All heating and cooling scans were at a rate of 10°C min^{−1}. Glass transitions (T_g) were taken as an average of the three mid-points for each cycle. Propellant formulation samples were tested in duplicate, with the standard deviation between the averages for the samples reported.

3 | Results and Discussion

3.1 | Thermo-mechanical Analysis

The viscoelastic properties of unfilled SEBS were compared with cured unplasticised HTPB using DMA (Figure 1—left). The storage modulus of SEBS was found to be generally much higher (+400%) than the HTPB sample, at 20°C. This denotes that SEBS is a stiffer material in comparison to HTPB, which would make it harder to deform. SEBS has two $\tan \delta$ peaks at −41 and +102°C due to the glass transition of the different blocks. The lower glass transition (T_{g1}) is due to the ethylene/butylene block, and the upper (T_{g2}) is caused by the styrene block. The lower glass-rubber transition is substantially at a higher temperature than the glass-rubber transition for HTPB ($\tan \delta$ maxima at −64°C), which may limit the propellants’ use for extreme cold conditions. The $\tan \delta$ also reports the amount of damping; between T_{g1} and 50°C, the $\tan \delta$ for SEBS is of similar magnitude to HTPB and greater above 50°C. However, due to the higher loss modulus (E'') of SEBS, the amount of energy being dissipated into the material would be higher.

For the AP/SEBS formulations (Figure 1—right), there is a clear increase in the storage modulus (above T_{g1}) as the solid filler (AP) of the formulation is increased, due to the reinforcement effect of the hard filler in the binder [12]. Below T_{g1} , the relationship is more complicated; this is likely to be due to the high storage modulus of the SEBS, while reducing its proportion in the formulation would decrease the modulus, the increased reinforcing effect of the additional filler would increase it. This should be investigated further.

DMA $\tan \delta$ curves (Figure 1—bottom right) show that the presence of the filler has an effect on the glass transition. Looking at the determined glass transition points (Table 3 and Figure 2), T_{g1} is similar to unfilled SEBS in most of the AP/SEBS formulations except for the highest solid-loaded sample (AP/SEBS (84/16)), which is ~2°C higher than unfilled SEBS. Conversely, T_{g2} is seen around 11°C lower for all the formulation samples. A similar complicated relationship between the shifting glass transition and filler has been seen in research with some other composites [13, 14]. It is believed to be due to the interaction between the polymer and the solid hard filler, causing restrictions to the

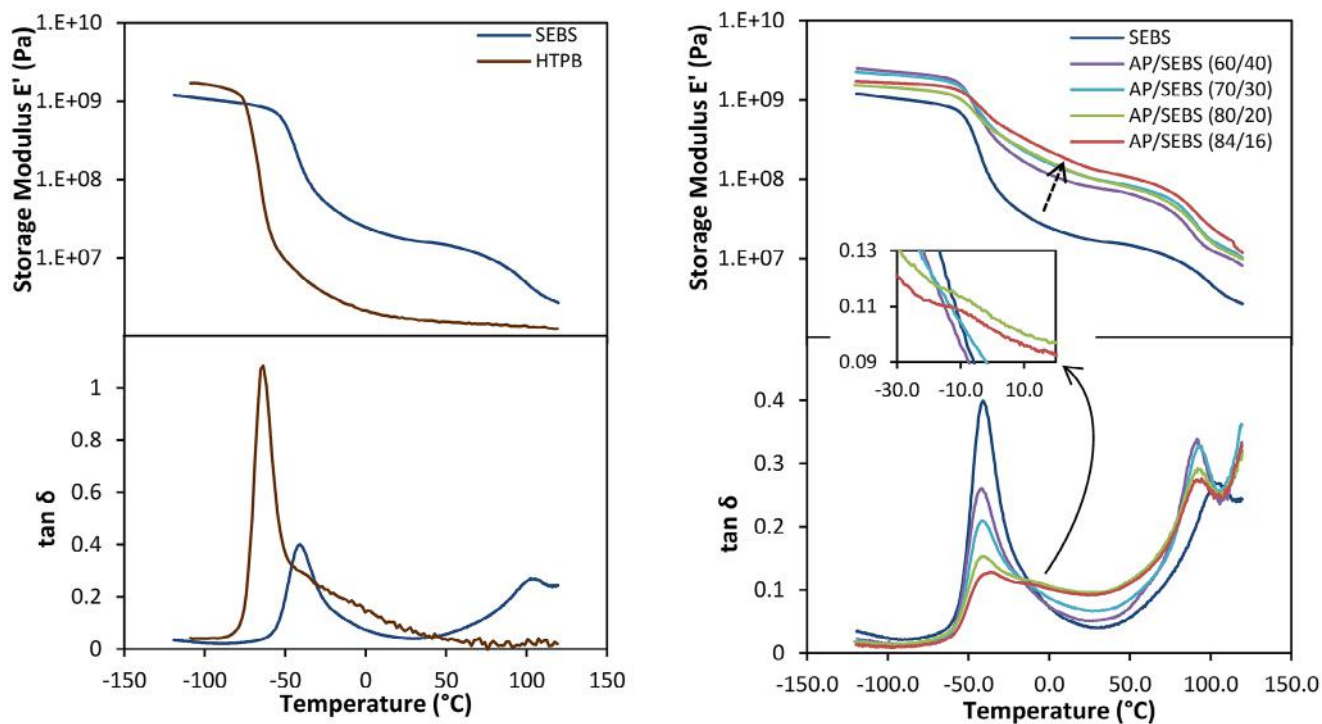


FIGURE 1 | Storage modulus (E') and loss factor ($\tan \delta$) dynamic mechanical analysis (DMA) thermogram at 1 Hz for (left) styrene-ethylene/butylene-styrene (SEBS) and cured hydroxyl-terminated polybutadiene (HTPB), and (right) ammonium perchlorate (AP)/SEBS propellant formulations and binder (SEBS). Zoomed in section (middle right), highlighting a small peak on AP/SEBS (80/20) and AP/SEBS (84/16). Results showing the loss modulus (E'') can be found in the supporting information (Figures S6 & S7).

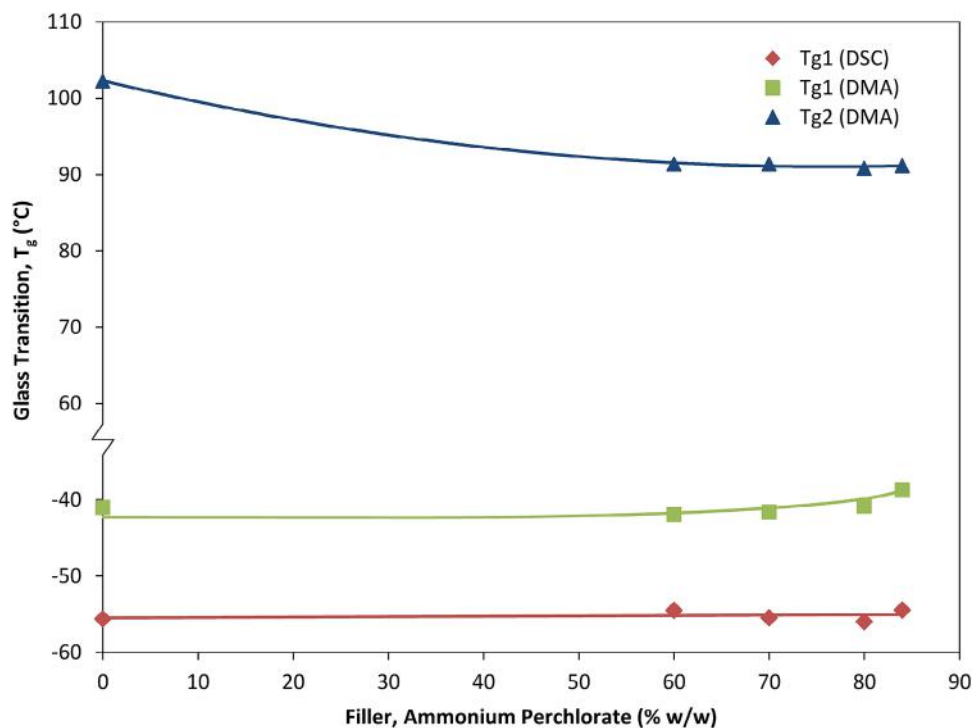


FIGURE 2 | Comparison of glass transitions for ammonium perchlorate/styrene-ethylene/butylene-styrene (AP/SEBS) propellant formulations for various solids loadings (AP) and unfilled SEBS found by differential scanning calorimetry (DSC) and dynamic mechanical analysis (DMA). Note that the upper glass transition (T_{g2}) was not detected by DSC.

TABLE 3 | Lower (T_{g1}) and upper (T_{g2}) glass transition for propellant formulation samples and unfilled binders (styrene-ethylene/butylene-styrene [SEBS] and cured hydroxyl-terminated polybutadiene [HTPB]), calculated from the $\tan \delta$ curve (1 Hz) and differential scanning calorimetry (DSC) (mid-point). Propellant formulation samples were in duplicate, with one standard deviation reported. DSC thermograms can be found in the supporting information (Figures S1–S5).

Sample	DMA		DSC
	T_{g1} (°C)	T_{g2} (°C)	T_{g1} (°C)
Unfilled SEBS	−41.0	102.3	−55.6 ± 0.0
Unfilled cured HTPB	−63.9	—	−74.6
AP/SEBS (60/40)	−41.9 ± 0.2	91.4 ± 0.9	−54.5 ± 0.2
AP/SEBS (70/30)	−41.6 ± 0.2	91.4 ± 0.7	−55.5 ± 0.0
AP/SEBS (80/20)	−40.8 ± 0.9	90.7 ± 0.5	−56.0 ± 1.9
AP/SEBS (84/16)	−38.7 ± 1.0	91.2 ± 1.3	−54.5 ± 1.0
RDX/SEBS (80/20)	−45.3 ± 0.3	90.6 ± 0.0	−55.6 ± 0.4

mobility of the polymer. As such, it would be expected to affect only the polymer near the particle-polymer interface; however, this appears to have more of a bulk effect on the composite. As this effect would appear to restrict the motion of the polymer, it would be expected to increase the glass transition temperature. However, it is believed that due to the nature of this interfacial interaction, the glass transition can also be shifted to a lower temperature.

A small new peak is visible around -10°C for the higher solids loading of AP/SEBS (80/20 and 84/16) in the $\tan \delta$ curve (Figure 1—right, zoomed in section). A similar peak with AP/HTPB propellants has been reported [6]. This is believed to be due to a rigid layer of polymer formed around the filler particle due to the interactions between AP and HTPB. This interaction could reduce the mobility of SEBS to such an extent that another glass transition occurs at a higher temperature in the higher solid-loaded samples.

All AP/SEBS formulation samples had a storage modulus (E') considerably greater than that of an AP/HTPB propellant, primarily due to increased modulus of the binder (SEBS) itself. For example, Cerri et al. [15] reported Storage Modulus, $G' = \sim 4 \times 10^6$ Pa at 20°C for AP/Al/HTPB/DOA (72/12/10.72/4% w/w plus other additives).

DMA analysis was also conducted on the RDX/SEBS (80/20) formulation, which was compared to AP/SEBS (80/20) (Figure 3). Similar-shaped thermograms were obtained for both the storage modulus and $\tan \delta$. Clearly, the storage modulus (E') is greater for the RDX formulation at all measured temperatures, especially above the lower glass transition temperature (T_{g1}). This is again due to the reinforcement effect of the hard filler in the binder; however, this effect is greater for the RDX formulation than AP, because of its smaller particle size. This results in a larger surface area in contact with the polymer, leading to a greater reinforcement effect [12].

The peak temperatures on the $\tan \delta$ graph were used to calculate the glass transition temperatures (Figure 3 and Table 3). T_{g1} for

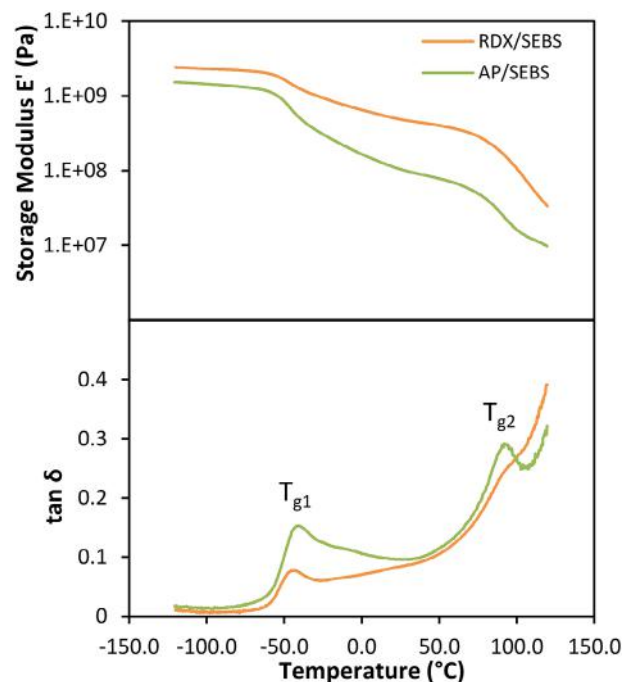


FIGURE 3 | Dynamic mechanical analysis (DMA) thermogram for ammonium perchlorate/styrene-ethylene/butylene-styrene (AP/SEBS) (80/20) and 1,3,5-trinitro-1,3,5-triazinane (RDX)/SEBS (80/20) propellant formulations, showing storage modulus, E' (top) and $\tan \delta$ (bottom) at 1 Hz. Results showing the loss modulus (E'') can be found in the supporting information (Figure S8).

the RDX/SEBS formulation was -45°C , which was noticeably different from the equivalent AP/SEBS formulation (-41°C), which saw almost no change from the unfilled SEBS sample. Changing the particle size and shape is believed to alter the interaction between the filler and binder, shifting the glass transition temperature [13]. Conversely, the effect on T_{g2} was very similar to the equivalent AP formulation, both around 91°C .

Only the lower glass transition for SEBS was detected by DSC (Table 3). This was determined for both AP/SEBS and RDX/SEBS formulations and compared against an unfilled pressed sample of SEBS. The glass transition determined by DSC was not expected to be influenced by the presence of a filler, unlike the result from mechanical analysis. The surface interaction of filler-polymer would only directly affect a very small amount of the total polymer, too small to be seen by DSC. This was found to be the case, with results between -55 and -56°C for the glass transition point, this difference being within error for the technique.

The storage modulus curves of frequency scans taken at differing temperatures (example in supporting information (Figure S9)) were shifted using the TTS principle to create a master curve [16]. From the reference temperature ($T_0 = 0^\circ\text{C}$), the curves were shifted to overlap; where they did not overlap, the curves were extrapolated. Ideally, the curves should all be overlapping without extensive extrapolation of the data; unfortunately, our data was generated from isotherms at 10°C intervals due to the limitation of the instrument. Repeating with additional isotherms at $1\text{--}2^\circ\text{C}$ intervals would be ideal. The master curve of the storage modulus (E') seems to fit, but the loss modulus (E'') and $\tan \delta$ do not.

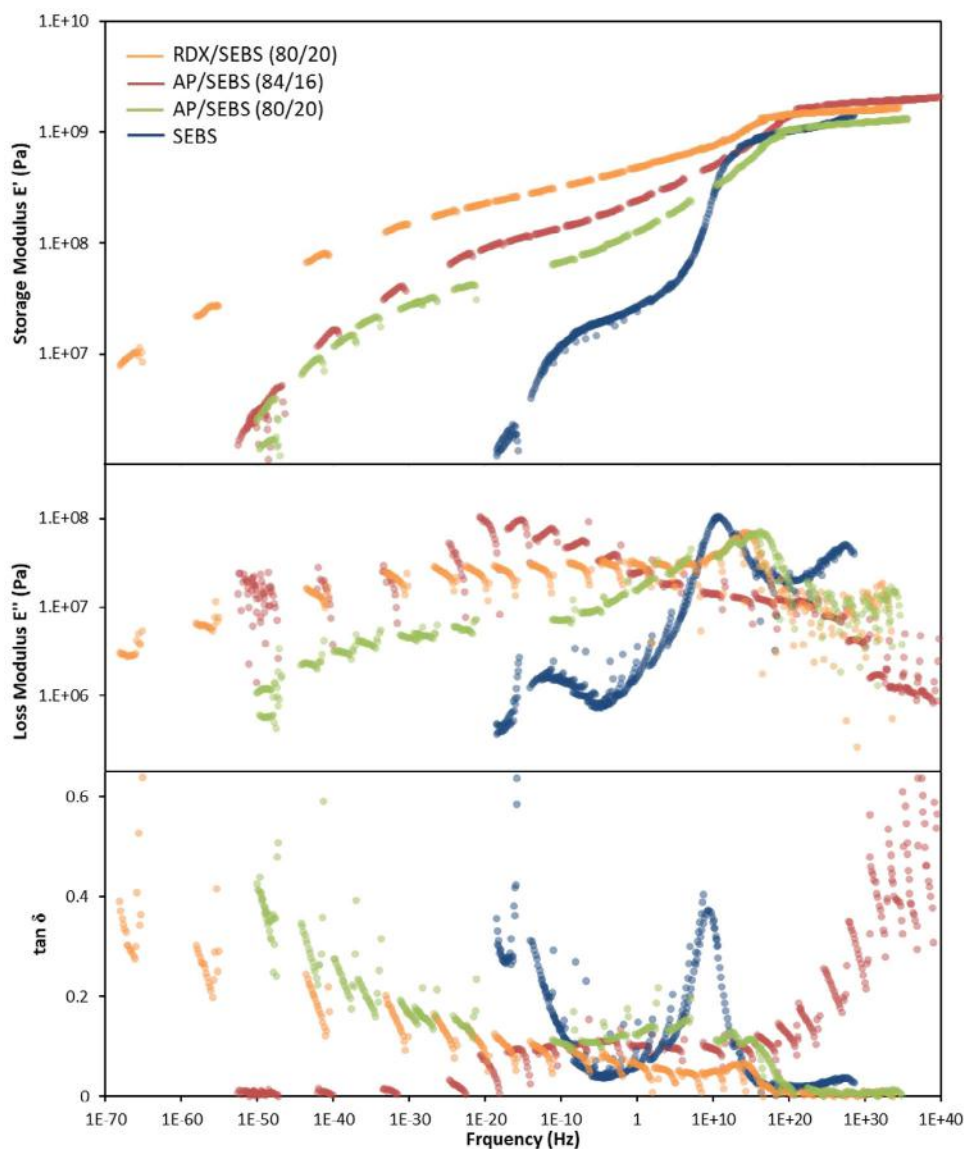


FIGURE 4 | Dynamic mechanical analysis (DMA) master curve of the storage modulus, E' (top); loss modulus, E'' (middle) and $\tan \delta$ (bottom) for 1,3,5-trinitro-1,3,5-triazinane/styrene-ethylene/butylene-styrene (RDX/SEBS) (80/20), ammonium perchlorate (AP)/SEBS (84/16) and AP/SEBS (80/20) propellant formulations, and unfilled SEBS. Reference temperature $T_0 = 0^\circ\text{C}$. On the storage modulus (E') graph. The master curves (storage modulus, E' and $\tan \delta$) for the other AP/SEBS propellant formulations can be found in the supporting information (Figure S10).

This indicates that we are outside of the valid range of the TTS extrapolation. This may be a result of the samples being partially crystalline, cross-linked and highly filled, therefore indicating that TTS might not be applicable.

The master curves for unfilled SEBS and selected propellant formulation samples are shown in Figure 4. The master curve for the storage modulus (E') gets flatter and wider with the addition of filler to the SEBS polymer. This indicates that as the solids loading increases, the storage modulus (E') changes less with frequency. The central region of the storage modulus is representative of the working range of the polymer. This spreading over the widest range of frequencies results in the greatest range in which the polymer stays in its rubbery state.

The different effect of the finer RDX filler can also be seen (Figure 4), with the same mass of filler flattening out the storage

modulus (E') even more than the same mass (80%) of AP. Presumably, this is due to the increased surface area, as seen with the lower glass transition (T_{g1}).

3.2 | Uniaxial Tensile Testing

Tensile testing of AP/SEBS propellant formulations (Table 4 and Figure 5) showed a general decrease in Young's modulus (E) and maximum stress (σ_{\max}) as the temperature is increased for all solids loadings. These trends are explained by Plaseied et al. [17] as being due to the increase in molecular mobility at higher temperatures, resulting in reduced stiffness (modulus), greater polymer ductility (maximum strain) and reduced maximum stress. The relationship between the strain at maximum stress (ϵ_m) and solids loading appears to be more complicated. As expected for a polymer, ϵ_m increases from -40 to $+20^\circ\text{C}$; however,

TABLE 4 | Uniaxial tensile testing of propellant formulation samples at -40 , $+20$ and $+74^\circ\text{C}$. Results are an average of five tests, with one standard deviation reported.

-40°C			
Sample	E (MPa)	σ_{\max} (MPa)	ϵ_m (%)
AP/SEBS (60/40)	203.4 ± 30.7	5.50 ± 0.74	8.5 ± 3.9
AP/SEBS (70/30)	281.3 ± 38.9	4.90 ± 0.30	4.0 ± 0.9
AP/SEBS (80/20)	235.9 ± 85.6	4.71 ± 0.49	3.1 ± 0.3
AP/SEBS (84/16)	223.1 ± 88.0	3.85 ± 1.24	2.4 ± 0.3
AP/HTPB Propellant (lit.) ^a	8.6	1.20	47
RDX/SEBS (80/20)	219.4 ± 29.5	8.05 ± 0.85	4.0 ± 0.2
$+20^\circ\text{C}$			
Sample	E (MPa)	σ_{\max} (MPa)	ϵ_m (%)
AP/SEBS (60/40)	87.1 ± 25.4	2.56 ± 0.41	135.6 ± 289.2
AP/SEBS (70/30)	151.4 ± 6.1	2.59 ± 0.26	4.1 ± 0.8
AP/SEBS (80/20)	135.7 ± 37.4	2.99 ± 0.13	2.8 ± 0.4
AP/SEBS (84/16)	161.9 ± 28.3	2.13 ± 0.21	1.8 ± 0.3
AP/HTPB Propellant (lit.) ^a	3.5	0.73	34
RDX/SEBS (80/20)	181.0 ± 52.3	3.62 ± 0.46	2.8 ± 0.4
$+74^\circ\text{C}$			
Sample	E (MPa)	σ_{\max} (MPa)	ϵ_m (%)
AP/SEBS (60/40)	55.1 ± 17.0	1.48 ± 0.14	11.5 ± 5.9
AP/SEBS (70/30)	59.3 ± 16.8	1.45 ± 0.12	6.6 ± 3.3
AP/SEBS (80/20)	66.0 ± 10.0	1.26 ± 0.42	3.1 ± 0.4
AP/SEBS (84/16)	92.6 ± 36.0	1.04 ± 0.40	1.9 ± 0.4
AP/HTPB Propellant (lit.) ^{a,b}	1.7	0.39	26
RDX/SEBS (80/20)	169.5 ± 47.0	2.46 ± 0.48	3.4 ± 0.3

^a2017_Adel,Guo-Zhu [19]; ^bLiterature sample conducted at 76°C .

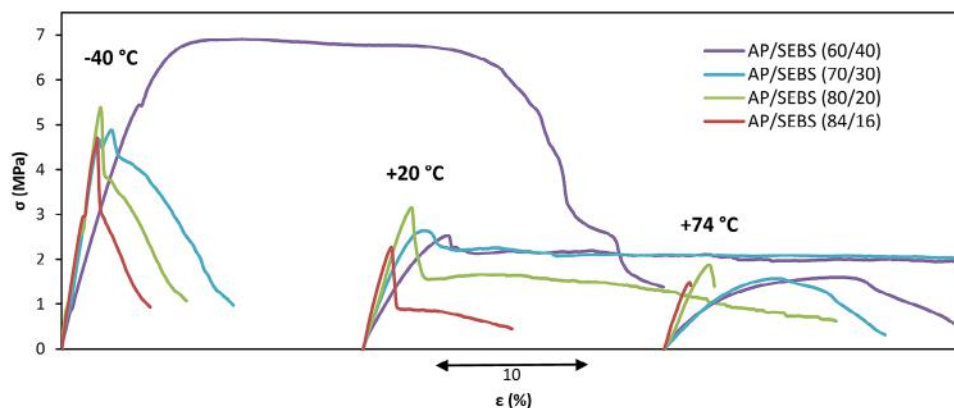


FIGURE 5 | Examples of uniaxial tensile testing results for ammonium perchlorate/styrene-ethylene/butylene-styrene (AP/SEBS) propellant formulation samples, showing stress (σ) against strain (ϵ), see supporting information for full results (Figures S11 and S12).

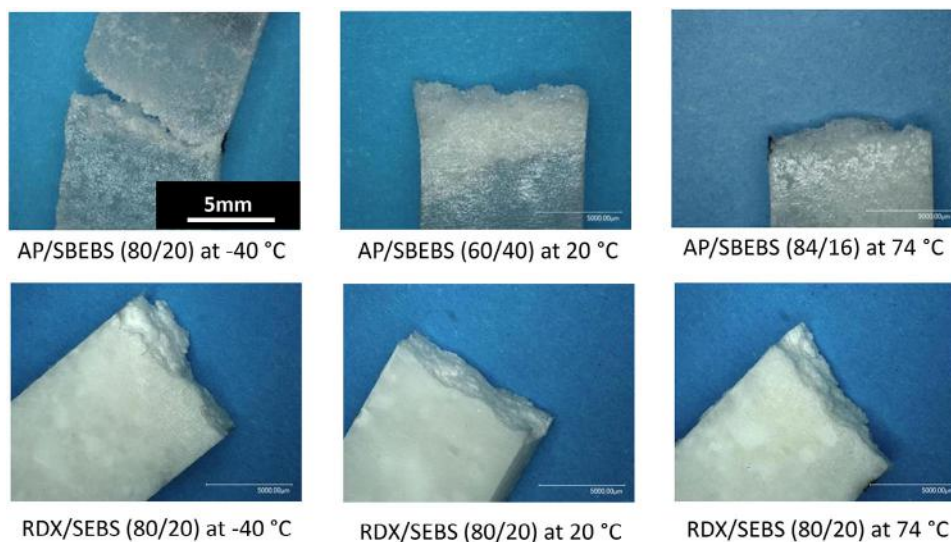


FIGURE 6 | Examples of test samples after tensile testing. More examples can be found in the supporting information (Figure S13).

it then decreases again at +74°C. This can be explained by the ‘fugitive’ cross-links that hold the structure of SEBS together. At +74°C, we are approaching the upper glass transition (T_{g2}) for SEBS, at which point these ‘fugitive’ cross-links begin to break. This makes the polymer less elastic and more viscous in behaviour, reducing ϵ_m .

At +20°C and +74°C, E increases with solids loading; at lower temperatures (−40°C), E increases then decreases with higher solids loading. Reducing the percentage of SEBS at low temperature, with its high modulus, becomes the more dominant effect over the reinforcing effect associated with increasing the solids loading [18], resulting in the overall Young’s modulus decreasing. With increasing solids loading, σ_{max} decreases slightly; this is due to the reduction in the percentage of binder being partially balanced out by an increasing reinforcing effect. The strain at maximum stress (ϵ_m) decreases rapidly with increasing percentage of filler. This is due to the solid rigid filler hindering the ductile behaviour of the polymer and the reduction in percentage of the binder. The ϵ_m results for AP/SEBS (60/40) at 20°C contained a large amount of variation. The extremely long elongation was due to the large proportion of binder in this formulation. However, the low solids loading causes an inhomogeneous formulation, resulting in some samples breaking earlier than others.

The effect of ductile behaviour of the propellant formulation sample can be seen in the images of the test samples after breaking (Figure 6). The lowest solids loading (AP/SEBS (60/40)) sample tested at +20°C underwent ductile fracture, which is shown by the whitening of the polymer as it has been stretched and ‘necked’. With higher solids loading and both lower (−40°C) and higher (+74°C) temperatures, the ductile behaviour is reduced, resulting in a brittle fracture.

In comparing the mechanical properties of AP/SEBS (86/14) propellant formulation to the literature, we need to consider two main factors: (1) the stiffness or modulus at 40–60°C to determine if the propellant charge can support its shape and form under dynamic loading. Bonding the propellant to a case lining can

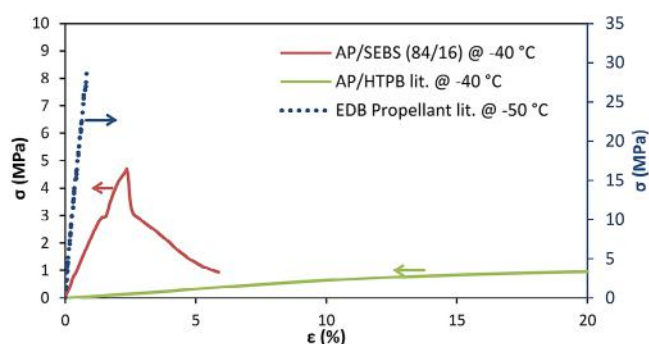


FIGURE 7 | Uniaxial tensile testing result for ammonium perchlorate/styrene-ethylene/butylene-styrene (AP/SEBS) (84/16) compared to extruded double base (EDB) Propellant lit., Shekhar [7] and AP/hydroxyl-terminated polybutadiene (HTPB) propellant lit., Adel and Liang [19], showing stress (σ) against extension (ϵ). EDB propellant is plotted on the secondary Y-axis (right) for clarity.

help support a weaker propellant. (2) The elongation or strain energy of the propellant in the cold state (−60 to −30°C) is important for understanding composite de-wetting and cracking. In order to compare the formulation sample AP/SEBS (84/16) with a traditional composite propellant, data reported by Adel and Liang [19] on tensile testing of HTPB-based composite propellants (67% AP, 18% Al and 15% HTPB) was utilised. From this reference, E , σ_{max} , and ϵ_m (Table 4), and strain energy density (Table 5) have been calculated by the author from graphical data. The AP/SEBS formulation has a greater Young’s modulus (E) and maximum stress (σ_{max}) than the AP/HTPB propellant. The strain at maximum stress (ϵ_m) is far less for AP/SEBS (84/16) at all temperatures measured. However, the strain extension at the breaking point is much closer to that of the AP/HTPB propellant. The AP/SEBS (86/14) formulation is closer in stiffness (modulus) and potential application to an extruded double base (EDB) propellant (Figure 7).

The low temperature strain energy density of the AP/SEBS (86/14) formulation was poor by comparison to the literature (Table 5). With further optimisation, such as the use of bonding agents,

TABLE 5 | Strain energy densities calculated from tensile testing. Results are an average of five tests, with one standard deviation reported.

Sample	Strain Energy Density to Maximum Stress, U_{\max} (kJ/m ³)		
	-40°C	20°C	74°C
AP/SEBS (60/40)	367 ± 233	388 ± 650	126 ± 76
AP/SEBS (70/30)	116 ± 31	69 ± 17	68 ± 37
AP/SEBS (80/20)	71 ± 7	45 ± 7	28 ± 10
AP/SEBS (84/16)	41 ± 16	21 ± 4	13 ± 5
AP/HTPB Propellant (lit.) ^a	456	84	61 ^b
RDX/SEBS (80/20)	152 ± 16	60 ± 11	54 ± 12

^a2017 Adel and Liang [19]; ^bLiterature sample conducted at 76°C.

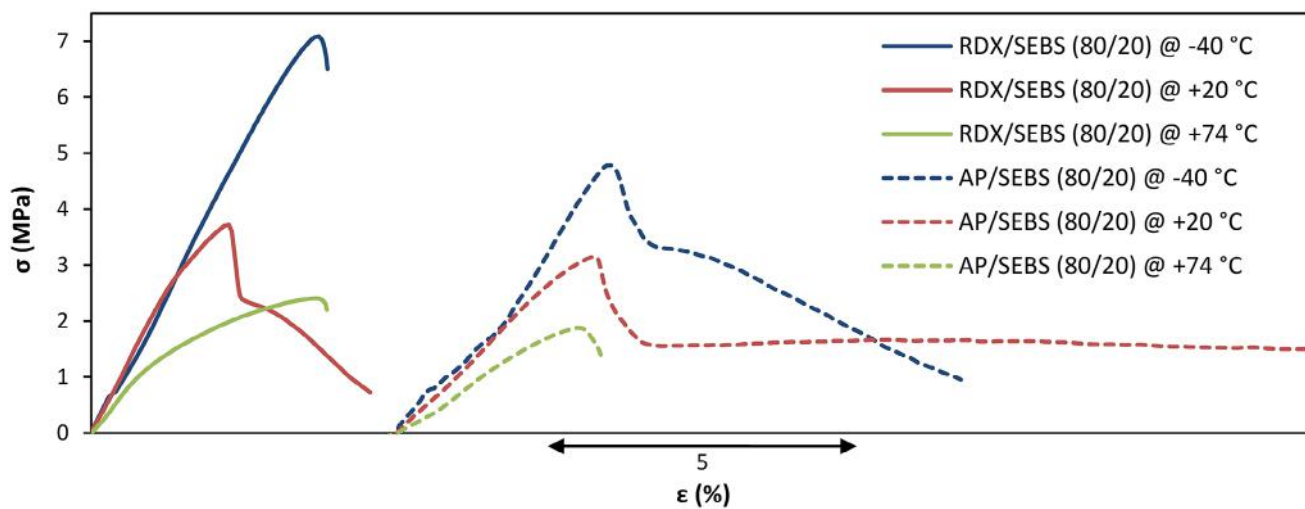


FIGURE 8 | Examples of uniaxial tensile testing results for 1,3,5-trinitro-1,3,5-triazinane/styrene-ethylene/butylene-styrene (RDX/SEBS) (80/20) compared to ammonium perchlorate (AP)/SEBS (80/20) samples, showing stress (σ) against strain (ϵ).

plasticisers, and optimised particle size, we believe the high modulus of the SEBS polymer can be exploited to significantly increase the strain energy capability of the propellant, to match or exceed that of an EDB propellant. Significant further optimisation would be required to enable the SEBS propellant formulation to be used in a high-performance case-bonded application. But the mechanical properties of an SEBS propellant formulation are expected to be suited to a cartridge-loaded grain or igniter charge.

For the RDX/SEBS formulation in Table 4, there is a trend of decreasing Young's modulus (E) and maximum stress (σ_{\max}) with increasing temperature. The strain at maximum stress (ϵ_m) appears to peak around room temperature. These are the same trends as seen with the AP/SEBS formulations.

By comparing the two propellant formulation samples, RDX/SEBS (80/20) with AP/SEBS (80/20) (Figure 8), the effect of the two fillers can be revealed. The RDX being finer in particle size in comparison to the AP has resulted in a tensile modulus E being greater for samples measured at +20 and +74°C. This is due to the greater reinforcement effect of the increased number of particles. ϵ_m has also decreased in comparison to AP/SEBS. This is probably due to the mono-modal distribution of RDX, as opposed to the bimodal distribution of the AP, resulting in an area between the particles being too large for the binder

to completely fill [9, 20]. Combined with the smaller particles of RDX, this results in a thinner layer of the binder between particles. At all temperatures, RDX/SEBS (80/20) undergoes brittle fracture (Figure 6). The increase in the maximum stress (σ_{\max}) is harder to explain; it is possibly due to the different particle size or a possible increased interaction between the filler and the binder. Behera [21] showed that by adding RDX in AP/HTPB propellant from 0 to 25%, E and ϵ_m both decreased, and σ_{\max} increased. This mirrors the effects of replacing AP with RDX reported in this paper.

4 | Conclusion

From a range of AP/SEBS and RDX/SEBS propellant formulations manufactured by a novel RAM slurry coating technique, thermal and mechanical analysis showed that the glass transitions (T_g) were only slightly changed from unfilled SEBS. In comparison to literature values of AP-composite propellants, both the storage modulus (E') from DMA and Young's modulus (E) from tensile testing were substantially greater. The maximum stress (σ_{\max}) was similar; however, the strain at maximum stress (ϵ_m) was less. The SEBS propellant formulation is closer in stiffness (modulus) and potential application to an extruded double base (EDB) propellant.

With further optimisation, such as the use of bonding agents, plasticisers, optimised particle size and improved manufacturing methods, it is believed that the maximum strain could be increased. Therefore, a SEBS-based propellant should deform less to an applied force and may have an elasticity approaching a HTPB composite propellant.

An optimised SEBS-based propellant could potentially meet the requirements for a low-cost, recyclable, sustainable propellant for a free-standing propellant grain as used in an ignitor or gas generator application.

Acknowledgements

We would like to thank Cranfield University, in particular Prof Jackie Akhavan, for supporting this PhD. Daniel Jubb at The Falcon Project Ltd for his ongoing support and help with LabRAM formulation and development, and to Defence Equipment & Support (DE&S, UK MoD) for funding the procurement of the LabRAM at Cranfield University.

Data Availability Statement

The authors have nothing to report.

References

1. "ITAR & Export Controls." Accessed: May 02, 2024, Available: https://www.pmdtc.state.gov/ddtc_public/ddtc_public?id=ddtc_public_portal_itar_landing.
2. "Understanding REACH." Accessed: May 02, 2024, Available: <https://echa.europa.eu/regulations/reach/understanding-reach>.
3. D. M. Moore, S. Young, P. Ito, K. Burgess, and P. Antill, "U.S. Export Controls and Technology Transfer Requirements—A United Kingdom Perspective," *International Journal of Defence Acquisition and Management* 3 (2010): 23.
4. M. Sloan and B. Wall, "Rocket Propellant Characteristics as Influenced by Cellulose Type and Source," in *3rd Nitrocellulose Symposium* (2007).
5. M. Hoffman, T. Hawkins, G. Lindsay, R. Wardle, and G. Manser, "Clean, Agile Alternative Binders, Additives and Plasticizers for Propellant and Explosive Formulations," in *Life Cycles of Energetic Materials* (1994).
6. J. A. Brydson, *Thermoplastic Elastomers—Properties and Applications*. Rapra Review Reports (Rapra Technology Ltd, 1995).
7. H. Shekhar, "Effect of Temperature on Mechanical Properties of Solid Rocket Propellants," *Defence Science Journal* 61, no. 6 (2011): 529–533, <https://doi.org/10.14429/dsj.61.774>.
8. A. Davenas, *Solid Rocket Propulsion Technology* (Pergamon Press, 1993).
9. G. P. Sutton and O. Biblarz, *Rocket Propulsion Elements, Ninth Edition* (John Wiley and Sons, 2017).
10. P. J. Wilkinson, M. C. Weaver, G. Kister, and P. P. Gill, "Styrene-Ethylene/Butylene-Styrene (SEBS) Block Copolymer Binder for Solid Propellants," *Propellants, Explosives, Pyrotechnics* 47, no. 1 (2022): 1–10, <https://doi.org/10.1002/prop.202100142>.
11. M. A. Bohn and S. Cerri, "Ageing Behaviour of Composite Rocket Propellant Formulations Investigated by DMA, SGA and GPC," *NDIA 2010 Insensitive Munitions & Energetic Materials Technology Session* 9, no. October (2010): 1–32.
12. D. Skelhorn, "Particulate Fillers in Elastomers," in *Encyclopedia of Polymers and Composites*, ed. R. Rother (Rapra Technology Limited, 2003), https://doi.org/10.1007/978-3-642-37179-0_9-1.
13. C. G. Robertson, C. J. Lin, M. Rackaitis, and C. M. Roland, "Influence of Particle Size and Polymer–Filler Coupling on Viscoelastic Glass Transition of Particle-Reinforced Polymers," *Macromolecules* 41 (2008): 2727–2731, <https://doi.org/10.1021/ma7022364>.
14. K. J. Lee, D. K. Lee, Y. W. Kim, W.-S. Choe, and J. H. Kim, "Theoretical Consideration on the Glass Transition Behavior of Polymer Nanocomposites," *Journal of Polymer Science, Part B: Polymer Physics* 45 (2007): 2232–2238, <https://doi.org/10.1002/polb>.
15. S. Cerri, M. A. Bohn, K. Menke, and L. Galfetti, "Ageing Behaviour of HTPB Based Rocket Propellant Formulations," *Central European Journal of Energetic Materials* 6, no. 2 (2009): 149–165.
16. K. Menard, "Frequency Scans," in *Dynamic Mechanical Analysis* (CRC, 2008), <https://doi.org/10.1201/9781420049183.ch7>.
17. A. Plaseied and A. Fatemi, "Strain Rate and Temperature Effects on Tensile Properties and Their Representation in Deformation Modeling of Vinyl Ester Polymer," *International Journal of Polymeric Materials and Polymeric Biomaterials* 57, no. 5 (2008): 463–479, <https://doi.org/10.1080/00914030701729677>.
18. H. L. Ornaghi, A. Bolner, R. Fiorio, A. J. Zattera, and S. C. Amico, "Mechanical and Dynamic Mechanical Analysis of Hybrid Composites Molded by Resin Transfer Molding," *Journal of Applied Polymer Science* 118, no. 2 (2010): 887–896, <https://doi.org/10.1002/app32388>.
19. W. M. Adel and L. Guo-zhu, "Analysis of Mechanical Properties for AP/HTPB Solid Propellant Under Different Loading Conditions," *International Journal of Aerospace Engineering* 11, no. 12 (2017): 1915–1919.
20. H. J. H. Brouwers, "Particle-Size Distribution and Packing Fraction of Geometric Random Packings," *Physical Review E: Statistical, Nonlinear, and Soft Matter Physics* 74, no. 3 (2006): 1–15, <https://doi.org/10.1103/PhysRevE.74.031309>.
21. S. Behera, "Effect of RDX on Elongation Properties of AP /HTPB Based Case Bonded Composite Propellants," *DRDO Science Spectrum* no. March (2009): 31–36.

Supporting Information

Additional supporting information can be found online in the Supporting Information section.

Supporting File 1: prep70067-sup-0001-SuppMat.docx